J. Phys. B: At. Mol. Opt. Phys. **23** (1990) 1175-1195. Printed in the UK

X-ray photoelectron, Auger electron and ion fragment spectra of O_2 and potential curves of O_2^{2+}

M Larsson†, P Baltzer‡, S Svensson‡, B Wannberg‡, N Mårtensson‡, A Naves de Brito‡, N Correia‡, M P Keane‡, M Carlsson-Göthe‡ and L Karlsson‡

† Manne Siegbahn Institute of Physics, S-104 05 Stockholm, Sweden
‡ Department of Physics, Uppsala University, Box 530, S-751 21 Uppsala, Sweden

Received 13 October 1989

Abstract. The O_2^{2+} ion has been studied by means of electron-impact-induced and photon-induced Auger electron spectroscopy and oxygen ion fragment spectroscopy of O_2. The oxygen ion kinetic energy spectrum was recorded by inverting the relevant potentials of an electron spectrometer for the detection of positive particles. The $^4\Sigma^-$ and $^2\Sigma^-$ O 1s initial core hole states have been studied using monochromatised x-ray photoelectron spectroscopy. Potential energy curves for a number of electronic states of the O_2^{2+} dication have been calculated with the complete active space SCF (CASSCF) and multireference contracted CI (MRCCI) methods with a one-particle basis set of medium size ([8s, 6p, 2d]). An analysis of the O_2 Auger electron spectrum based on the computed potential curves of O_2^{2+} is presented. The autoionisation satellites are analysed and it is found that these lines correspond to molecular singly ionised final states. One line at 510.7 eV, however, is associated with an atomic-like transition. Two shake-up Auger satellites are identified by a comparison with a recent O 1s shake-up spectrum from O_2.

1. Introduction

Spectroscopy of doubly charged molecular ions has been an active field of research in recent years (Mathur 1988). Despite this, experimental information regarding the structure and spectroscopy of doubly charged molecules is sparse. This is due to their short lifetimes, high reactivity and a general sparsity of bound electronically excited states, which makes it difficult to apply spectroscopic techniques relying on transitions between bound electronic states. In fact, only two doubly charged molecules have been studied in some detail by means of high-resolution spectroscopy, namely N_2^{2+} (Carroll 1958, Cossart *et al* 1985, Cossart and Launay 1985, Olsson *et al* 1988) and NO^{2+} (Cossart *et al* 1987) by optical spectroscopy, and N_2^{2+} (Cosby *et al* 1983, Sarre 1989) by fast beam laser spectroscopy. The majority of doubly charged molecular ions have been explored by means of techniques that are inherently of low resolution (Eland *et al* 1988, Mathur 1988) or by theoretical calculations.

The O_2^{2+} dication, which is of particular interest for its potential influence on the properties of the ionosphere, has been investigated by a large variety of techniques over the years such as Auger electron spectroscopy (Siegbahn *et al* 1969, Moddeman *et al* 1971), mass spectrometry (Dorman and Morrison 1963, Märk 1975), ion kinetic energy spectroscopy (Beynon *et al* 1971, Brehm and de Frenes 1978, Curtis and Boyd 1984), photoion-photoion coincidence (PIPICO) spectroscopy (Curtis and Eland 1985,

0953-4075/90/071175+21$03.50

Eland *et al* 1988), energy gain spectroscopy (Pedersen 1986) and double charge transfer spectroscopy (Appell *et al* 1973). Very recently, the double charge transfer (DCT) spectrum of O_2^{2+} was reinvestigated (Fournier *et al* 1989) at a higher resolution than in the earlier experiment (Appell *et al* 1973) and several new features were observed. Fluorescence from O_2^{2+} following soft x-ray-induced core electron ionisation has recently been claimed (Tohji *et al* 1986, Yang *et al* 1988). This observation has not yet been confirmed by a coincidence technique (e.g. photoion-photon of fluorescence coincidence, Besnard *et al* 1986) or by rotational analysis of the observed fluorescence. It is no exaggeration to state that no coherent picture of the structure and spectroscopy of O_2^{2+} emerges from the experiments described above.

Theoretical calculations of potential curves are scarce. Hurley (1962) used the spectroscopic data of N_2, which is the corresponding isoelectronic neutral system, in order to predict the potential curves of O_2^{2+}. The number of curves calculated by Hurley was limited by the available information about the corresponding states in N_2. Beebe *et al* (1976) performed minimal basis full valence CI calculations of a large number of potential curves of O_2^{2+}. More recently, Fournier *et al* (1989) have performed SCF-CI calculations of O_2^{2+} in order to facilitate the analysis of the double charge transfer spectrum of O_2^{2+}. CI calculations were performed also by Yang *et al* (1989) in order to find support for the assignment of the x-ray-induced optical emission spectrum of O_2^{2+} (Tohji *et al* 1986, Yang *et al* 1988). The agreement between the different calculated results is poor. For example, Hurley (1962) and Yang *et al* (1989) predict the $A^3\Sigma^+$ state, which may be the lower state in the transition giving rise to the alleged O_2^{2+} emission, to be bound, while Beebe *et al* (1976) and Fournier *et al* (1989) predict this state to be purely repulsive.

The Auger electron spectrum of O_2 has been, in a convincing manner, reinterpreted by Sambe and Ramaker (1986) partly on the basis of the calculations by Hurley (1962), and by Dunlap *et al* (1981) using $X\alpha$ calculations. In view of the objections to the results of Hurley (1962) that follow from some of the *ab initio* calculations (Beebe *et al* 1976, Fournier *et al* 1989) and the fact that $X\alpha$ calculations cannot distinguish the various multiplet states arising from an electronic configuration, we decided to make a complete reinvestigation of the Auger spectrum of O_2. Electron spectroscopy studies were performed by means of both electron beam and photon excitation in high-resolution electron spectrometers. Moreover, the ion kinetic energy spectrum was recorded by inverting the relevant potentials of the electron spectrometer in order to allow for the detection of positive particles (in this case atomic oxygen ions). In order to have reliable potential curves for the interpretation of the Auger spectrum, *ab initio* calculations of the potential curves of O_2^{2+} were carried out with the complete active space SCF (CASSCF) and multireference contracted CI (MRCCI) methods.

The double ionisation energies $I^{2+}(i)$, related to particular electronic states (i), are obtained as the difference between the ionisation energy of the initial core hole state, $I^+(1s)$, and the kinetic energy E_A of the electron emitted in the KVV (core-valence, valence) Auger process, that is

$$I^{2+}(i) = I^+(1s) - E_A \tag{1}$$

assuming that interaction between the Auger electron and the emitted core electron can be neglected. The latter energies are obtained from the Auger electron spectrum, while the former have been determined by x-ray photoelectron spectroscopy.

Since the oxygen molecule has an open shell with a π^2 electron configuration in the neutral ground state, photoionisation from the O 1s orbital leads to two multiplet

states of $^4\Sigma^-$ and $^2\Sigma^-$ symmetry with different energies. Although the core level photoelectron spectrum of the oxygen molecule has been studied earlier by several groups, we have made a new high-resolution study in order to determine the energies of the two multiplet components accurately and also to observe the lineshapes. A difference in the linewidths and lineshapes of the $^4\Sigma^-$ and $^2\Sigma^-$ states would be expected if the equilibrium bond distances for the two multiplet states were different as has been predicted theoretically by Ågren *et al* (1978, 1979) performing ΔSCF calculations. A difference of this kind could also lead to different linewidths in the Auger electron spectrum.

2. Experimental and theoretical details

2.1. Experimental details

The x-ray photoelectron spectra were recorded on a spectometer normally used for high-energy excitation. Monochromatised Al K_α radiation ($h\nu = 1487$ eV) was used for the excitation of spectra. The energies of the two O 1s multiplet components of O_2 were calibrated against the $^4\Sigma_u^-$ line in the valence region at 24.58 eV (Edqvist *et al* 1970). The photon-induced Auger spectrum was also obtained by means of this instrument. The Al K_α radiation was used for excitation of the Auger spectrum as well.

The electron-impact-excited Auger electron and ion fragment studies were carried out on an electron spectrometer designed for high-resolution UV-photoelectron and electron impact Auger electron spectrosocopy of gas phase samples (Baltzer *et al* 1989). In the present Auger electron investigation a 2 keV electron beam was used to create the initial O 1s core hole states. All spectra were recorded by varying the retardation/acceleration voltage between the sample cell and the analyser, while keeping the analyser voltage constant corresponding to a pass energy of 50 eV. The energy scale of the Auger electron spectra was calibrated against the strong $L_{2,3}MM$ Auger lines in argon at 201.09, 203.47 and 205.62 eV (Werme *et al* 1973). This calibration gives energy positions within 0.1 eV for the narrowest lines.

By reversing the polarities of all relevant voltages in the spectrometer, positively charged oxygen fragment ions due to dissociation of singly or doubly charged molecules could be studied. These studies were carried out using an analyser pass energy of 50 eV. In order to get high intensity at the multichannel detector, a post-acceleration voltage of 100 V was applied between the analyser and the front of the MCP detector. In our previous studies we have found that the zero-point energy in ion kinetic energy spectra is well represented by the crossing between the inflection point tangent of the low-energy edge of the line corresponding to very low energy fragments and the baseline. The energy scale of the present oxygen ion kinetic energy spectrum was assigned in this manner with an estimated accuracy of about ±0.2 eV.

2.2. Theoretical methods

The basis set for oxygen was derived from van Duijneveldt's (1971)(13s, 8p) primitive set augmented with two d functions. This primitive set was contracted to [8s, 6p, 2d] with the exponents and contraction coefficient for the innermost 6s, 3p and for the d functions taken from Lie and Clementi (1974). This basis set is expected to yield adequate accuracy while being sufficiently small to allow a large number of calculations to be performed. CASSCF calculations were performed using the Newthon–Raphson

method as described by Siegbahn *et al* (1981). The CASSCF active space was chosen to include the valence MO $2\sigma_g, 2\sigma_u, 3\sigma_g, 3\sigma_u, 1\pi_u$ and $1\pi_g$. The $1\sigma_g$ (O 1s) and $1\sigma_u$ (O 1s) orbitals were inactive, i.e. doubly occupied in all configurations. The active orbitals were defined as the natural orbitals. For computational reasons D_{2h} symmetry was used instead of $D_{\infty h}$ symmetry. A symmetry restriction was introduced by averaging the density matrices of the $\Pi_{u,x}$ and $\Pi_{u,y}$ symmetries and of the $\Pi_{g,x}$ and $\Pi_{g,y}$ symmetries. Apart from the singlet ground state $X^1\Sigma_g^+$, only triplet states were calculated since these states are the only ones that could be observed by Auger electron spectroscopy. The occurrence of $\Delta_{u,g}$ states requires some caution; it is otherwise easy to mistake a $\Delta_{u,g}$ for a $\Sigma_{u,g}^+$ or a $\Sigma_{u,g}^-$ state. For this reason, calculations on $\Delta_{u,g}$ states were, in cases where ambiguities could arise, carried out both in the Δ_{u,g,x^2-y^2} and $\Delta_{u,g,xy}$ symmetries at several different internuclear distances. In cases where a particular state was not the lowest of its symmetry, the energy of the appropriate root of the CAS CI secular equation was optimised. The CASSCF calculations were carried out at about 10–15 different internuclear distances.

In order to account for dynamical correlation effects, the CASSCF calculations were followed by multireference externally contracted CI (MRCCI) (Siegbahn 1983) calculations with the CASSCF wavefunctions as zero-order reference. Since the configuration expansions are very lengthy we considered reference configuration selection. Thus, configuration state functions (CSF) from the CASSCF were included as reference states only if the absolute value of the coefficient of one of their component spin couplings was above a threshold of 0.05 at least at one internuclear distance. The set of reference states for a particular electronic state was identical at all internuclear distances during the MRCCI calculations.

3. Results and discussion

3.1. The O 1s photoelectron spectrum

The electron configuration of the oxygen molecule in the neutral ground state is

$$(1\sigma_g)^2(1\sigma_u)^2(2\sigma_g)^2(2\sigma_u)^2(3\sigma_g)^2(1\pi_u)^4(1\pi_g)^2.$$

From this configuration three electronic states arise, namely $^3\Sigma_g^-$, $^1\Delta_g$ and $^1\Sigma_g^+$, where $^3\Sigma_g^-$ corresponds to the ground state. As was mentioned above, photoionisation from the core levels leads to two multiplet components $^4\Sigma^-$ and $^2\Sigma^-$. Figure 1 shows the photoelectron spectrum obtained in the present study. The splitting between the peak maxima of the two lines corresponding to the multiplet components is 1.11 eV, confirming results presented earlier (Gelius 1973). The binding energies were calibrated against the $^4\Sigma_u^-$ line in the valence region at 24.58 eV (Edqvist *et al* 1970) and are 543.37 and 544.48 eV, respectively. These values are approximately 0.3 eV higher than previously given values (Siegbahn *et al* 1969). The discrepancy is due to an error in the position of the CO_2 lines (Johansson *et al* 1973) used for the calibration of the spectrum by Siegbahn *et al* (1969).

As can be seen, the lines are asymmetric indicating that several vibrational levels are excited in the core hole states. The linewidths are also very different, 0.41 eV for the $^4\Sigma^-$ final state and 0.49 eV for the $^2\Sigma^-$ final state, indicating that the equilibrium bond distance of the two states is different. This agrees qualitatively with the theoretical results by Ågren *et al* (1978, 1979), who obtained bond distances of 1.276 and 1.331 Å, respectively, for these core hole states. It should be noticed that, according to Ågren's

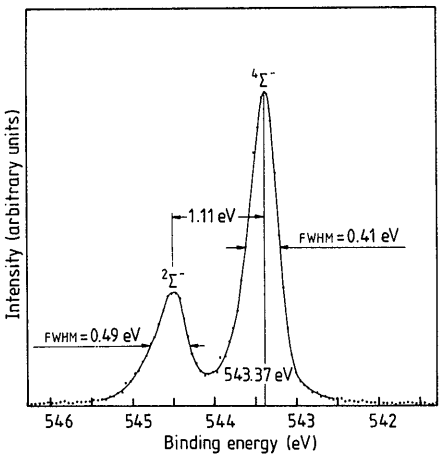

Figure 1. The O 1s photoelectron spectrum of O_2 excited by means of monochromatised x-rays at 1487 eV (Al Kα). The lines corresponding to the multiplet components are well resolved and show very different widths (FWHM).

calculations, the peak maximum of the $^2\Sigma^-$ final state corresponds to the $v=2$ vibrational component, whereas the peak maximum of the $^4\Sigma^-$ final state lies between the $v=0$ and $v=1$ components. These results are qualitatively confirmed by the observed band shapes, especially we note the low binding energy tail of the $^2\Sigma^-$ line. Therefore the adiabatic multiplet splitting should be approximately 0.2 eV smaller than the distance between the peak maxima in figure 1.

The ratio between the peak heights of the $^4\Sigma^-$ and $^2\Sigma^-$ components is 2.75, which is much larger than the statistical ratio of 2 for the ratio between the photoionisation cross sections. In the previous work by Sambe and Ramaker (1986) a ratio of 2.5 was quoted using experimental data from Siegbahn *et al* (1969) and Bagus *et al* (1974). However, since the linewidths are different, which has not been recognised earlier with non-monochromatised measurements at low resolution, the peak heights are not appropriate for determination of the ratio for the photoionisation cross section. If instead the areas of the photoelectron lines obtained in the present study are used, an intensity ratio close to the former published values could be obtained (cf figure 1). Theoretical studies of the intensity ratio between the quartet and the doublet states have been performed by Bagus *et al* (1974) and Darko *et al* (1977). Using correlated wavefunctions these authors calculated ratios of 2.28 and 2.40, respectively.

Ågren *et al* did not include the anharmonicity in their calculations and therefore we may in general expect a larger experimental intensity of the higher vibrational components. This implies that the progression from the $^4\Sigma^-$ final state may extend under the $^2\Sigma^-$ line. The intensity ratio is therefore difficult to establish and a more detailed study will be reported elsewhere in connection with similar studies on other small paramagnetic molecules.

3.2. The electron-impact- and photon-impact-excited Auger electron spectra

The electron-impact-excited Auger electron spectrum of the O_2 molecule between 440 and 520 eV kinetic energy obtained in the present study is shown in figure 2. It is

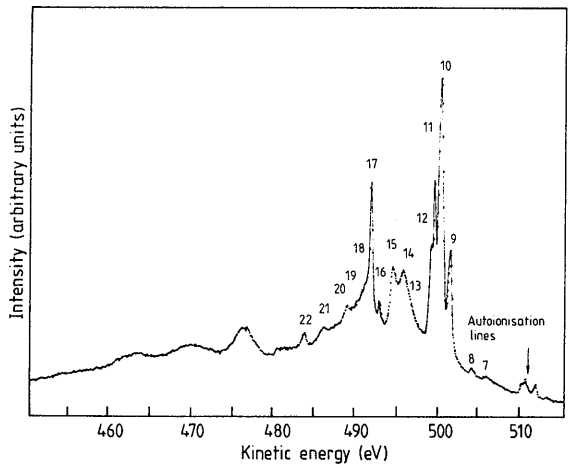

Figure 2. The electron-impact-excited KVV Auger electron spectrum of the O_2 molecule recorded between 450 and 515 eV kinetic energy. An enlargment of the autoionisation region is shown in figure 4. Details of the lines between 502 and 490 eV are shown in figures 6 and 7.

similar to spectra obtained previously (Siegbahn *et al* 1969, Moddeman *et al* 1971) but is recorded at somewhat higher resolution and with better statistics in order to establish the detailed features of the spectrum. The clearly discernible features are numbered from 1 to 22. The energies of the lines and assignments are summarised in table 1.

Figure 3 shows the photon-impact-excited Auger electron spectrum from 475 to 515 eV kinetic energy. This spectrum was earlier obtained by Moddeman *et al* (1971), however at lower resolution and signal to background ratio. The spectra of figure 2 and 3 are very similar at kinetic energies below 508 eV. Above this energy a series of weak lines are only observed in the electron-impact-excited spectrum.

3.2.1. The lines above 508 eV. The weak lines above approximately 508 eV are not observed in the photon-excited Auger electron spectrum. They can therefore be associated with autoionisation processes, leading to the single hole states reached also in photoelectron transitions from the ground state or excited states of the neutral molecule. As was discussed earlier by Sambe and Ramaker (1986) autoionisation probably takes place essentially from one highly excited state, the $1\sigma^{-1}1\pi^3(^3\Pi)$ state (the core-excited molecule should preferably be described in the $C_{\infty v}$ symmetry), which is reached in a transition from the O 1s($1\sigma_u$) orbital to the initially half-filled $1\pi_g$ orbital. Figure 4 shows a detailed recording of this spectrum. As for the O 1s core hole states observed in the photoelectron spectrum, the equilibrium geometry of the $^3\Pi$ core-excited initial state should differ significantly from that of the neutral ground state. The transitions to the final, singly ionised states are therefore expected to take place from different vibrational levels of the $^3\Pi$ state. The energies of the peak maxima are given in table 1. If these energies are subtracted from the energy for the $1\sigma^{-1}1\pi^3$ ($^3\Pi$) state we should obtain values corresponding to the lines of the valence photoelectron spectrum. The energy for the $1\sigma^{-1}1\pi^3$ ($^3\Pi$) state measured by electron energy loss and by photoabsorption is given in a report by Hitchcock and Brion (1980). However, different values are quoted ranging from 529.9 to 532 eV. If 530.17 eV is subtracted from the values for the lines 1–4 in table 1 we get energies in close agreement

Table 1. Experimental kinetic energies and assignments in terms of autoionisation and Auger electron transitions for the electron-impact-induced electron spectrum of O_2.

Line	Electron energy (eV)	Final state energy (eV)		Assignments
		$^4\Sigma^-$ initial state	$^2\Sigma^-$ initial state	
1	513.44			$^{1,3}\Pi_u \rightarrow a^4\Pi_u$
2	512.65			$^{1,3}\Pi_u \rightarrow A^2\Pi_u$
3	512.19			$^{1,3}\Pi_u \rightarrow b^4\Sigma_g^-$
4	511.34			$^{1,3}\Pi_u \rightarrow {}^2\Phi_u$
5	510.88			atomic-like
6	510.38			$^{1,3}\Pi_u \rightarrow {}^2\Delta_g$
7	506.23			
8	504.23			
9	501.64		42.8	$^2\Sigma^- \rightarrow W^3\Delta_u$
10	500.50	42.9		$^4\Sigma^- \rightarrow W^3\Delta_u$
11	499.73	43.6		$^4\Sigma^- \rightarrow B^3\Pi_g$
12	499.35	44.0		$^4\Sigma^- \rightarrow B'^3\Sigma_u^-$
13	496.79		47.7	$^2\Sigma^- \rightarrow C^3\Pi_u$
14	495.78	47.6		$^4\Sigma^- \rightarrow C^3\Pi_u$ and $1^3\Sigma_g^-$
15	494.62	48.8		$^4\Sigma^- \rightarrow 2^3\Pi_u$
16	492.94		51.5	$^2\Sigma^- \rightarrow 2^3\Sigma_g^-$
17	491.90	51.5		$^4\Sigma^- \rightarrow 2^3\Sigma_g^-$
18	491.03			
19	490.19			
20	488.94			
21	486.11			
22	483.76			

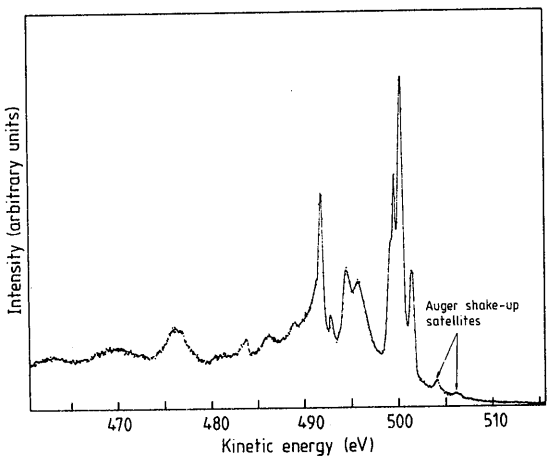

Figure 3. The photon-excited KVV Auger electron spectrum of the O_2 molecule recorded between 475 and 515 eV kinetic energy.

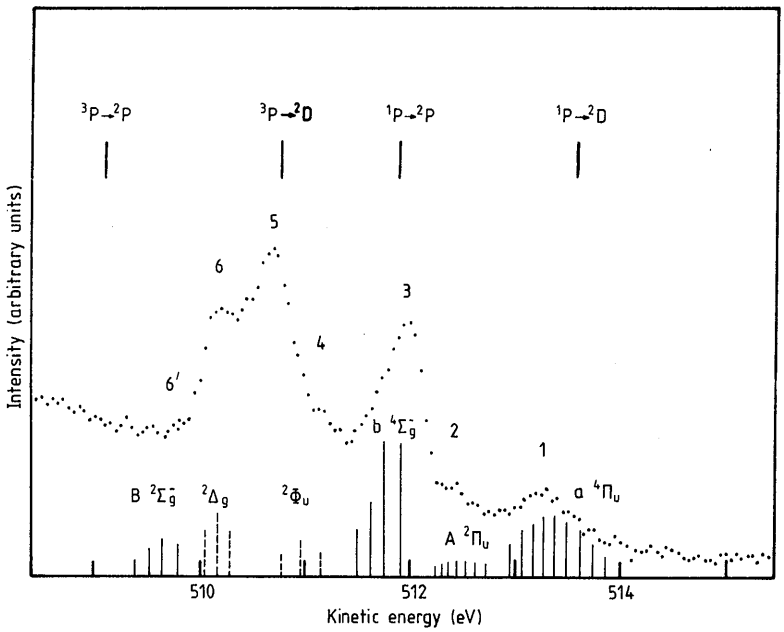

Figure 4. Detail of the electron-beam-excited O_2 Auger electron spectrum showing the autoionisation region between 509 and 515 eV. Lines 1,2,3,4,6 and 6′ can be assigned to processes involving singly ionised final states of the molecule. Line 5 has no molecular counterpart and is interpreted as originating from an atomic-like transition.

with the vertical binding energies in the He I excited photoelectron spectrum (Edqvist *et al* 1970, Jonathan *et al* 1974). Assignments of the lines 1–4 are inserted in table 1. These assignments are in accordance with the earlier assignments by Sambe and Ramaker.

The excitation paths are different for the autoionisation and the photoelectron spectra. The vibrational envelope of the different bands in the autoionisation spectrum may therefore be different from those of the corresponding bands of the photoelectron spectrum. However, for the band at 512 eV, corresponding to transitions to the b $^4\Sigma_g^-$ cationic state, a vibrational progression with approximately the expected spacings of 140 meV can be inferred from intensity variations on the low-energy side of line 3 in a highly resolved spectrum. This fact facilitates the assignment of this band. The lack of clear vibrational structure could be due to both a lifetime broadening of the initial state and transitions from different vibrational levels of the initial state.

The energy of line 6 coincides with the energy of the $^2\Delta_g$ state. It should be noticed that, due to an incorrect reproduction of the energy scale taken from Siegbahn *et al* (1969), Sambe and Ramaker assigned this state to line 5 (R6 in their figure 2). As a consequence of our assignment of the $^2\Delta_g$ state, the B $^2\Sigma_g^-$ state is assigned to the weak line 6′ in figure 4.

All possible states in the region 0–25 eV binding energy of O_2^+ have been observed by photoelectron spectroscopy except a $^2\Sigma_u^+$ and a $^2\Pi_u$ state (Jonathan *et al* 1974). According to calculations (compare Jonathan *et al* 1974) these states, however, fall at a larger energy than the B $^2\Sigma_g^-$ state. Thus a relative shift in the order of 1 eV would be needed if one of these states was assigned to line 5. Therefore such an assignment to line 5 of hitherto unobserved states is implausible.

Since no singly ionised molecular state can be associated with line 5 we therefore propose that it corresponds to an atomic-like transition as has been earlier observed by Morin and Nenner (1986), Aksela and Aksela (1989), Carroll and Thomas (1988), Cafolla *et al* (1989) and Svensson *et al* (1989). Using the arguments of Carroll and Thomas the core-ionised atom will effectively behave as a fluorine atom, which has a substantially smaller atomic radius. The orbitals can thus be described as atomic-like and the energy for the autoionisation process may be obtained primarily from atomic energies. Morin *et al*, however, propose a model in which the dynamical effects are considered, i.e. the neutral system dissociates into atomic fragments before the autoionisation process takes place.

The strongest satellite line in the Ne KLL Auger spectrum is the $1s2p^5(^3P)$–$2p^3(^2D)$ transition. We therefore expect that this transition should be strong also in the atomic oxygen core-excited autoionisation spectrum. The energy of this type of process has been estimated by us using a semiempirical procedure. The O 1s ionisation energy for atomic oxygen has been calculated to be 545.4 eV (Huang *et al* 1976). The correlation energy correction for the O 1s level can be estimated to be about 1.0 eV (Chen *et al* 1985). A first approximation of the O $1s\,2p^5$–O $1s\,2p^4$ energy difference is, according to the $Z+1$ approximation, 17.4 eV (Moore 1949). An $X\alpha$ procedure (Johansson and Mårtensson 1980) is used to calculate a correction to this energy which amounts to 0.6 eV. The estimated multiplet average energy of the $1s2p^5$ configuration is in this way $545.4+1.0-17.4-0.6=528.4$ eV. The ^1P–^3P splitting is estimated from the corresponding splitting in Ne of 4.4 eV (Svensson *et al* 1988). The splitting is obtained by rescaling according to the observed Z dependence of the corresponding $1s2p^1$ ^1P–^3P splitting (Moore 1949). This gives for the O $1s2p^5$ ^3P state an estimated energy of $528.4-\frac{1}{4}\times 2.8=527.7$ eV. The O $2p^3$ ^2D state has an energy of 16.9 eV (Moore 1949) which leads to a calculated transition energy of 510.8 eV, which is rather close to the experimental energy of peak 5 in figure 4. It should be mentioned that a structure around 511 eV is observed also in the oxygen autoionisation spectra from CO, CO_2 (Carroll and Thomas 1988, Moddeman *et al* 1971), COS (Carroll and Thomas 1988) and also in the NO spectrum a weak line can be seen (line A6 in Moddeman *et al* 1971). This supports the atomic character of this transition.

With this assignment the autoionisation spectrum contains lines of both molecular and atomic origin. A similar mixed behaviour was noted by Carroll and Thomas (1988) and has been observed also for HCl by Aksela and Aksela (1989). In the case of O_2 one might speculate that the $1\pi_g$ orbital, which is strongly antibonding, is responsible for this mixing. If the excited electron remains as a spectator in the autoionisation process, the final state will be atomic-like as for the initial state, whereas if this electron takes part in the transition the final state will be molecular. Such a speculation should be tested in an extensive calculation. This, however, falls outside the scope of this report.

A related phenomenon has recently been observed by Cafolla *et al* (1989) using synchrotron-radiation-excited photoelectron spectroscopy. These authors have observed atomic autoionisation processes in the valence shell when studying the O_2 molecule. They explain this by a very long lifetime (10^{-12}–10^{-13} s) for the autoionising Rydberg states, allowing the highly excited molecule to dissociate before the autoionising transition takes place. Their situation is, however, different from the one in this report where a core-excited oxygen molecule has been studied.

3.2.2. The DCT spectrum and the Auger spectrum below 502 eV. The strong lines appearing at kinetic energies lower than 502 eV are associated with the KVV Auger electron

transitions from the initial single hole states observed in the x-ray excited photoelectron spectrum in figure 1. The interpretation will be focused on the lines observed between 490 and 502 eV, which correspond to transitions to final states of O_2^{2+} that are considered in the calculations of the present study.

Since the two different initial electronic states are separated by 1.11 eV, the Auger electron spectrum is composed of two superimposed spectra separated by this energy. Pairs of lines, which are split by 1.1 eV and thus may correspond to transitions to the same final state, are (9, 10), (14, 15) and (16, 17). These identifications were also made in the study by Sambe and Ramaker (1986). However, the difference in equilibrium distance for the $^2\Sigma^-$ and $^4\Sigma^-$ core hole states complicates the pattern. In the case of a potential for the final state in the Auger transition that is steep and has a rapidly varying slope, this gives a substantial deviation from the 1.11 eV separation. For the single lines 11 and 12, the counterparts are obviously hidden under line 10.

Regarding the interpretation of the spectrum, it was pointed out by Sambe and Ramaker that the final states that can be reached in the Auger transition are governed by some selection rules. In the first place, pairs of lines corresponding to transitions from the $^4\Sigma^-$ and $^2\Sigma^-$ initial states can only be observed for transitions to triplet states, assuming that *LS* coupling applies. The reason is that the outgoing electron removes a spin of $\pm\frac{1}{2}$ from the system and the only common spin state for transitions from the $^4\Sigma^-$ and $^2\Sigma^-$ states is a triplet. Secondly, the final states cannot have Σ^+ symmetry, since the outgoing electron cannot have Σ^- symmetry.

For the interpretation of the Auger electron spectrum it is essential to compare also with the results from double charge transfer spectroscopy (DCT). A study has been performed by Appell *et al* (1973) using proton impact to create the doubly ionised states of oxygen. The following single-collision process was considered

$$H^+ + O_2 \rightarrow H^- + O_2^{2+}. \tag{2}$$

By measuring the kinetic energy distribution of the H^- ions, the double ionisation energies I^{2+} of the oxygen molecule could be obtained from the relation

$$I^{2+} = (E - E_0) - E(H^-) - T_m \tag{3}$$

where E is the experimentally determined energy of the H^- ions, E_0 is the initial kinetic energy of the protons and $E(H^-) = -14.3$ eV is the energy required to form H^- in its ground state from H^+. The recoil energy T_m was negligible under the experimental conditions used in this study. Due to the conservation of spin in the experiment, the doubly ionised states are expected to be formed with the same spin as the neutral ground state, that is, only triplet final states are expected. This was also found in the investigation by Appell *et al.* Thus in both the Auger and DCT spectra the transitions primarily involve triplet final states. In addition, approximate selection rules exist, which suppress the formation of O_2^{2+} in $^3\Sigma_u^+$ states as in the Auger electron spectrum. Thus, the $^3\Sigma_u^+$ state is observed only as a shoulder in the DCT spectrum by Appell *et al.* In a more recent and well resolved work (Fournier *et al* 1989), the $^3\Sigma_u^+$ state is observed as a peak at 41.1 eV, in good agreement with the present calculations.

One would thus expect a close correspondence between the lines observed in the DCT and in the Auger electron spectrum. This is corroborated by a comparison between the experimental data, which shows that all the lines of the former have a counterpart in the latter and vice versa. The lines in the spectra thus seem to be associated with transitions to triplet states of O_2^{2+}. We have therefore carried out calculations mainly on these states.

The calculated potential curves, corresponding to triplet states, are presented in figure 5. For completeness, the lowest electronic state $X\,^1\Sigma^+$ arising from the $1\pi_g^{-2}$ electron configuration and the $A\,^3\Sigma_u^+$ state from the $1\pi_u^{-1}1\pi_g^{-1}$ configuration of the dication have been included, although Auger transitions to these states are not expected to have an observable intensity. Also the centres of the Franck–Condon regions for transitions from the $^4\Sigma^-$ and $^2\Sigma^-$ initial states are shown, assuming that the centres correspond to the equilibrium bond distances of these states. In table 2 we give the state energies calculated at this internuclear distance along with the linewidths estimated by projecting a Franck–Condon region on the potential curves. By comparison with N_2^{2+}, for which very similar calculations were recently carried out (Olsson *et al* 1988), one would expect errors in the calculated energies of the order of 0.1–0.3 eV. The present curves are in qualitative agreement with those of Beebe *et al* (1976) and Fournier *et al* (1989). In general, the electronic states of O_2^{2+} cannot be associated with single-electron configurations but for a proper description substantial configuration mixing must be included. However, for guidance in the discussion we give the leading configurations for some different states.

3.2.3. Assignments of the Auger electron lines. Due to the selection rules, the lowest state that will become appreciably populated in Auger transitions is the $W\,^3\Delta_u$ state,

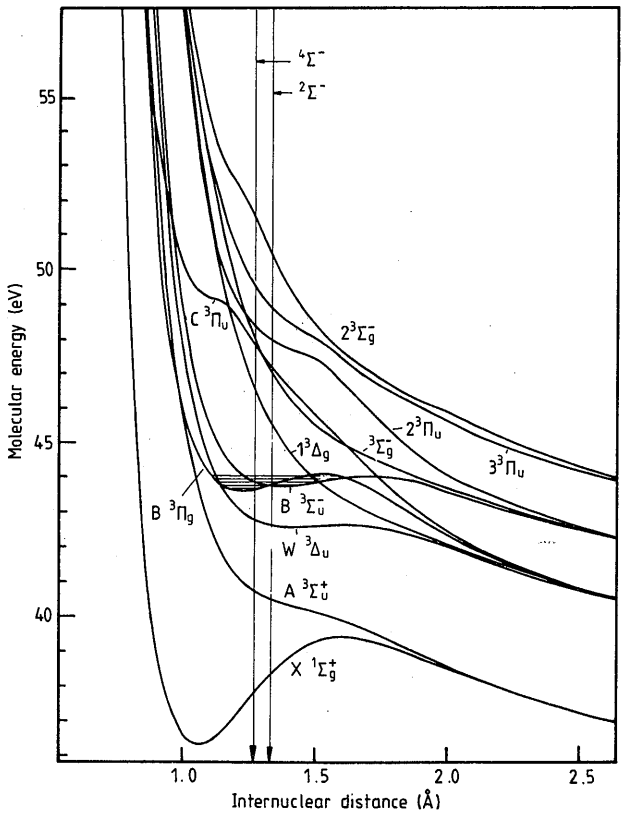

Figure 5. Potential energy curves of O_2^{2+} from CASSCF/MRCCI calculations. The notations of the electronic states follow those of Hurley (1962) and are related to the notations used for N_2^{2+}.

Table 2. Calculated energies for the electronic states of O_2^{2+} at the internuclear distances of 1.27 and 1.33 Å corresponding to the equilibrium bond distances of the $^4\Sigma_u^-$ and $^2\Sigma_u^-$ states, respectively. All energies are referred to the experimental value 42.9 eV for the W $^3\Delta_u$ state. Also the linewidths estimated for Franck-Condon transitions from the $^4\Sigma^-$ state are given.

Electronic state of O_2^{2+} (eV)	Energy		Linewidth (FWHM) (eV)
	$^4\Sigma_u^-$ initial state	$^2\Sigma_u^-$ initial state	
X $^1\Sigma_g^+$	37.8	38.3	
A $^3\Sigma_u^+$	40.7	40.5	
W $^3\Delta_u$	42.9	42.7	0.8
B $^3\Pi_g$	43.7	43.9	
B′ $^3\Sigma_u^-$	44.0	43.9	
$1^3\Delta_g$	46.5	45.5	2.2
$1^3\Sigma_g^-$	47.9	47.0	2.3
C $^3\Pi_u$	47.8	47.3	1.3
$2^3\Pi_u$	48.4	48.0	0.9
$3^3\Pi_u$	49.6	49.0	1.4
$2^3\Sigma_g^-$	51.7	50.7	1.8

primarily associated with a $1\pi_u^{-1}1\pi_g^{-1}$ electron configuration. The two intense lines at 500.5 and 501.6 eV, which are split by 1.16 eV, should thus correspond to transitions to this final state from the $^4\Sigma^-$ and $^2\Sigma^-$ initial states, respectively, as pointed out above. Due to the different Franck-Condon regions for transitions from the $^4\Sigma^-$ and $^2\Sigma^-$ initial states, the splitting deviates slightly from the value 1.11 eV observed in the x-ray photoelectron spectrum of the O 1s core levels. As expected, the $^4\Sigma^-$ transition gives rise to a more intense line than the $^2\Sigma^-$ transition. The Franck-Condon region falls on a sloping part of the potential curve, leading to a theoretically estimated linewidth (FWHM) of 0.75 eV. Figure 6 shows an enlarged part of the spectrum including the outermost Auger transitions. From this figure an experimental linewidth of 0.7 eV can be measured for both lines, in good agreement with the value obtained from the calculated potential curve.

The next line in the spectrum (number 11) is observed at 499.6 eV. Since there is no line at 1.1 eV lower kinetic energy in the Auger electron spectrum, this line must correspond to the low energy transition from the $^4\Sigma^-$ state, while the transition from the $^2\Sigma^-$ initial state is hidden under the intense line 10 at 500.5 eV. According to the calculated energies line 11 is due to transitions to the $(3\sigma_g^{-1}1\pi_g^{-1})$ B $^3\Pi_g$ final state. The line is very narrow. From the spectrum shown in figure 6 the width can be estimated to be only about 0.3 eV, which shows that the vibrational broadening must be small. This agrees with the calculated results, where the centre of the Franck-Condon region falls near the equilibrium bond distance for this state (cf figure 5). The transition from the $^2\Sigma^-$ initial state, which we place under line 10, should be broader as can also be seen from figure 5.

Also line 12 observed in the spectrum at 499.3 eV should have a counterpart that is hidden under the peak maximum of line 10. The calculations suggest that this line corresponds to transitions to the $(1\pi_u^{-1}1\pi_g^{-1})$ B′ $^3\Sigma_u^-$ state. The centre of the Franck-Condon region meets the potential curve at a slightly lower energy than the observed energy of line 12 (cf figure 5 and tables 1 and 2). Line 12 is much broader than 11, the estimated linewidth being about 0.6 eV. Thus the equilibrium bond distance is

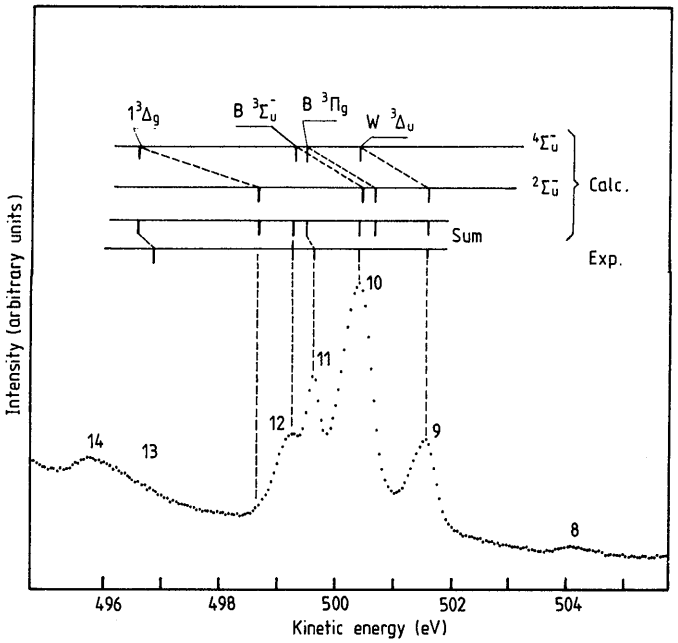

Figure 6. Detail of the electron-impact-excited O_2 Auger electron spectrum showing the energy region around 500 eV at high resolution. Transition energies from the calculations are inserted as a bar diagram.

expected to differ greatly from that of the B $^3\Pi_g$ state. This is in agreement with the calculations, which give an internuclear equilibrium distance of about 1.37 Å for the B' $^3\Sigma_u^-$ state (cf figure 5), i.e. much larger than the equilibrium distance 1.27 Å of the $^4\Sigma^-$ initial state. The next final state is predicted to have $^3\Delta_g$ symmetry with a leading $1\pi_u^{-2}$ electron configuration. This state is strongly repulsive with a large slope in the Franck-Condon region (cf figure 5). From the figure the linewidth can be estimated to be about 2.2 eV. Thus, the transitions are expected to give rise to two very broad bands with low peak intensity. These obviously contribute to the broad and asymmetric structure observed with maximum intensity at 496 eV. The structures corresponding to the transitions to the $^3\Delta_g$ state are unresolved but we tentatively place them at 496.6 eV (structure 13) and 498.7 eV, since the intensity at the latter energy is higher than expected from the background alone. Especially in the photon-induced spectrum this background is seen to be very low. It should be noticed that, due to the very steep slope of the potential curve for this state (cf figure 5), the splitting between the components associated with the $^2\Sigma^-$ and $^4\Sigma^-$ core hole states is not 1.11 eV since the Franck-Condon regions fall at different internuclear distances.

The inner part of the Auger spectrum considered in the present calculations is shown in figure 7. The outermost line at 496 eV is the same line as shown in figure 6. As was mentioned above, calculations were performed only for the region with energies higher than 490 eV. The lines at lower energies have strong contributions from inner valence orbitals of O 2s character.

The high energy part of the structure 14 at 496 eV obviously gets intensity from more transitions than the one to the $^3\Delta_g$ state discussed above. However, the calculations suggest that transitions from the $^2\Sigma^-$ initial state to the C $^3\Pi_u$, $2^3\Pi_u$, $3^3\Pi_u$ and $(1\pi_u^{-2})1^3\Sigma_g^-$ final states give the predominant contribution to the intensity in this region,

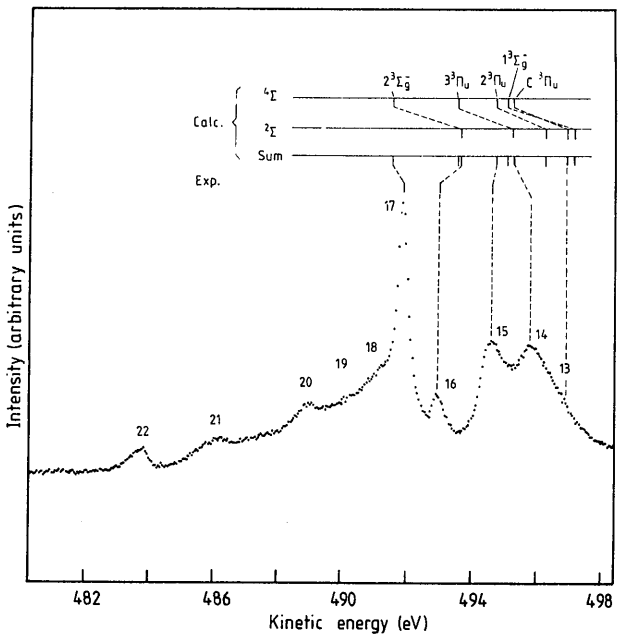

Figure 7. Detail of the electron-impact-excited O_2 Auger electron spectrum showing the energy region around 490 eV at high resolution. Transition energies from the calculations are inserted as a bar diagram.

as can be seen from figure 5. The corresponding transitions from the $^4\Sigma^-$ initial state to the higher energy states should contribute to the central parts of bands 14 and 15. In particular, band 14 can be associated with the C $^3\Pi_u$ and $1^3\Sigma_g^-$ final states (cf also next section) while band 15 probably corresponds to transitions to the $2^3\Pi_u$, $3^3\Pi_u$ final states. Since the transitions to the $1^3\Sigma_g^-$ final state should give rise to a very broad structure (cf table 2) the peak maximum of band 14 is probably mainly due to transitions to the C $^3\Pi_u$ state.

The splitting of 1.18 eV between lines 14 and 15 corresponds essentially to the splitting between the two initial states $^4\Sigma^-$ and $^2\Sigma^-$. Since the lines are broad, primarily due to the large slope of the potential curves in the Franck-Condon regions, they may well contain somewhat different contributions from the final states listed above and with a splitting of 1.11 eV between the initial states. The comparatively high intensity of line 14 is also partly due to contributions from the transitions to the $^3\Delta_g$ state discussed above.

The spacing of 1.14 eV between the narrow lines 16 and 17 at 493.0 and 491.9 eV, respectively, indicates that these lines correspond to transitions to the same final state. As can be seen from figure 7, the weaker line 16 is broader than line 17. The linewidths can be estimated from the figure to be 0.7 and 0.5 eV, respectively, which gives an intensity ratio of the order of 2.8 between the two transitions if the areas are considered. Obviously the broad structure 18 extends under line 17 which contributes to the apparent high intensity of the latter line. The difference in linewidth can partly be explained by the difference in equilibrium bond distance between the core hole states. As was seen above, the transitions to the core hole states tend to populate higher vibrational levels of the $^2\Sigma^-$ initial state than of the $^4\Sigma^-$ initial state. Since the Franck-Condon region for transitions from the higher vibrational levels is broader

than from the lower, transitions from the $^2\Sigma^-$ state may give rise to broader Auger electron bands than from the $^4\Sigma^-$ state. Furthermore, variations in both the linewidth and energy spacings between the two components can arise due to the fact that the Franck–Condon regions are centred at different bond distances. To explain the small linewidth, particularly of line 17, a much smaller slope in the Franck–Condon region is required than is calculated for the remaining $(3\sigma_g^{-2})2^3\Sigma_g^-$ final state potential curve that can be associated with lines 16 and 17. However, the required behaviour is shown in figure 5 although the small slope occurs at a smaller internuclear distance than the Franck–Condon region. The plateau that can be seen for the $2^3\Sigma_g^-$ final-state potential curve at about 1.22 Å internuclear distance obviously originates from the interaction between this state and other $^3\Sigma_g^-$ final states. It is possible that the configuration mixing is not fully described by the calculation, leading to locally incorrect potential curves for the different states possessing this symmetry. The assignment is tentative since there are other strongly repulsive potential curves in the same energy region that are not shown in figure 5. The assignment of peaks 13–17 does not agree with that given previously by Sambe and Ramaker.

For the broad structures numbered 18–22, transitions involving holes in orbitals with O 2s character have to be considered in the calculations. In the present study we have not performed such calculations where correlation and also interference effects make the assignment complicated.

3.2.3. The lines 7 and 8. If we compare the electron-impact-induced spectrum of figure 2 with the photon-induced spectrum of figure 3 we immediately see that the autoionisation lines 1–6 disappear in the latter figure. However, lines 7 and 8 are present in both spectra and must therefore be associated with an Auger process. The energies of these lines do not agree with the calculated normal Auger energies for transitions to the $X\ ^1\Sigma_g^+$ and $A\ ^3\Sigma_u^+$ final states. Therefore these lines must be assigned to Auger shake-up satellite processes where the shake-up electron in the Auger initial state takes part in the Auger transition. All other satellite processes lead to low kinetic energy satellites. This agrees with the interpretation made by Sambe and Ramaker (1985).

The analysis of lines 7 and 8 therefore calls for an analysis of the O 1s core shake-up spectrum from O_2. A recent high-quality shake-up spectrum has been obtained by Nordfors *et al* (1989). In this spectrum we find a dominating shake-up structure at about 10 eV shake-up energy. This line was interpreted as originating from π_u–π_g shake-up processes. A close inspection of this line reveals at least three components at 552.0, 553.6 and 555.9 eV binding energy with the approximate relative intensities of 0.8 : 1 : 0.1, respectively. The $1\sigma^{-1}\pi_u^{-1}\pi_g^3$ shake-up configuration contains three states: $^2\Sigma^-$, $^4\Sigma^-$ and $^2\Sigma^-$. The doublets interact with the doublet core hole and the quartet with the quartet core hole. With the observed shake-up energies we therefore obtain consecutive splittings between the $1\sigma^{-1}\pi_u^{-1}\pi_g^3$ shake-up states of 1.6 and 2.4 eV, respectively (cf figure 8). In this figure we have also included the experimental energies for the singly ionised O 1s core hole states and the energy of the common $1\sigma^2\pi_u^{-2}\pi_g^2$ final state. The possible states that can be reached in an Auger transition within this configuration are $1^3\Sigma_g^-$ and $1^3\Delta_g$. We have earlier assigned line 13 to the $1^3\Delta_g$ state whereas the $1^3\Sigma_g^-$ contributes to line 14. The satellites 7 and 8 can be used to further strengthen this assignment since, if we assume that the $1^3\Delta_g$ state is the final state, we obtain a main line Auger energy which is 0.9 eV too high. The remaining possibility is a $1^3\Sigma_g^-$ final state which thus obtains an experimental energy of 47.6 eV. The weak $^2\Sigma^-$ component at 555.9 eV is probably not observed as an Auger satellite. The

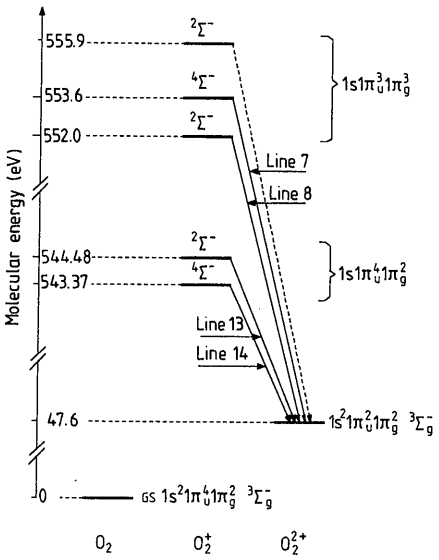

Figure 8. Energy levels involved in the shake-up Auger satellite transitions (lines 7 and 8 in figure 2) and the corresponding main line transitions (13 and 14 in figure 2). The O 1s shake-up and main line energies are obtained from a recent high resolution x-ray photoelectron study (Nordfors *et al* 1989).

assignment of the lines 7 and 8 above thus follows the arguments made earlier by Sambe and Ramaker with the exception that the satellite final state has $^3\Sigma_g^-$ symmetry instead of $^3\Delta_g$ symmetry.

3.3. The electron-impact-induced ion fragment spectrum

When the target molecules are exposed to the intense electron beam, singly, doubly and more highly ionised molecules are created in various electronic states. Dissociation from such states leads to ion fragments that may possess high kinetic energies. In previous studies of hydrogen halides it has been found that the ion spectra primarily are due to dissociation from singly and doubly ionised molecules (Baltzer *et al* 1988, 1989) whereas more highly charged atoms give smaller contributions. The doubly ionised systems were found to be created both by direct two-electron emission and by Auger electron transitions, where the former process tended to dominate.

The kinetic energy release is obtained as the difference between the energy of the initial molecular ionic state and the energy of the final state given by the separated fragments. The initial state energy is dependent on the position of the Franck–Condon region for the transition in which it was created. This implies that for the dicationic states of the oxygen molecule, which are created by direct double ionisation and two Auger processes that have somewhat different Franck–Condon regions, predissociative initial states are created with three slightly different energies. This will be manifested in the ion spectrum as a broadening of the individual lines.

Figure 9 shows the ion fragment spectrum for oxygen obtained with an electron beam energy of 1500, 300 and 100 eV. Six rather broad structures can be discerned with kinetic energies up to about 6.5 eV as shown in the figure. Above this energy a broad distribution extends up to at least 10 eV kinetic energy. All energies have been

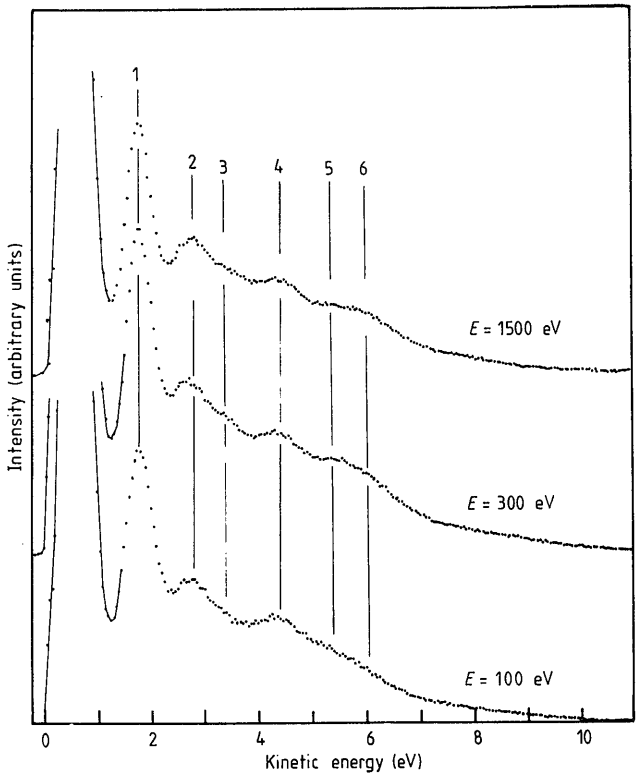

Figure 9. The ion kinetic energy spectrum following 1.5 keV, 300 eV and 100 eV electron impact on O_2.

measured for ionised oxygen atoms, which implies that the energies released in the dissociation are twice as large. The energies 300 and 100 eV are both well below the threshold for Auger transitions which occur slightly above 540 eV (cf above). Nevertheless, the spectra are practically the same as that obtained at 1500 eV suggesting, as for the hydrogen halides in previous studies, that the most important contributions to these spectra come from direct two-electron transitions.

Table 3 summarises the energies and assignments of the structures observed in the spectrum. In figure 10 we have extended the potential curves for the doubly ionised molecule to the limit of separated atoms or ions. The energies for the various separated systems that correlate with the molecular states have been calculated from the dissociation energy 5.12 eV of neutral O_2 in its ground state and the ionisation energies for atomic oxygen. From these data and the energies of the dicationic states determined from the Auger spectrum, ion fragment energies for a number of states have been calculated. The energies for the $X\,^1\Sigma_g^+$ and $A\,^3\Sigma_u^+$ states, which are not observed in the Auger spectrum, have been taken from the calculated potential curves. These ion fragment energies, which were determined for an internuclear distance between the centres of the two Franck-Condon regions for the Auger transitions, are also given in table 3.

The structures 3 and 4 are well described by dissociation of doubly ionised molecules. However, the experimental energies are somewhat higher than the calculated energies. This is further evidence that the direct double ionisation, which leads

Table 3. Kinetic energies and assignments for the electron-impact-induced ion fragment spectrum of O_2. The calculated energies are obtained as the difference in energy between the doubly ionised states observed (see text) and the separated fragments.

Line no	Kinetic energy (eV)	Assignment	Calculated energy (eV)
1	1.8		
2	2.8		
3	3.4	$B\,^3\Sigma_u^- \rightarrow O^+(^4S)+O^+(^2P)$	3.3
4	4.5	$B\,^3\Pi_g \rightarrow O^+(^4S)+O^+(^2D)$	4.0
		$A\,^3\Sigma_u^+ \rightarrow O^+(^4S)+O^+(^4S)$	4.3
5	5.4		
6	6.0	$1^3\Delta_g \rightarrow O^+(^4S)+O^+(^2D)$	6.0
		$1^3\Sigma_g^- \rightarrow O^+(^4S)+O^+(^2P)$	6.3
		$C\,^3\Pi_u \rightarrow O^+(^4S)+O^+(^2D)$	6.6
		$2^3\Pi_u \rightarrow O^+(^4S)+O^+(^2P)$	7.1

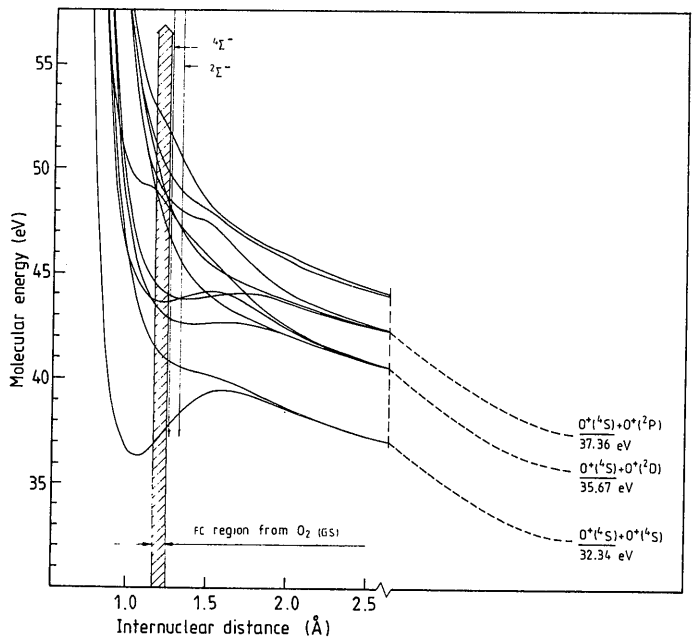

Figure 10. Potential energy curves illustrating the dissociation of the doubly ionised states of O_2. The Franck-Condon region for direct double ionisation is shown along with the centre of the Franck-Condon regions for the Auger initial core hole states. Using a Born-Haber cycle in this diagram the energies for the O^+ ions can be calculated. These energies are observed in the ion fragment spectrum of figure 9.

to higher energies than the Auger processes (cf figure 10), is important. In particular, the $A\,^3\Sigma_u^+$ state could only involve the former process since it is not reached in the Auger transitions. Also dissociation from the $B'\,^3\Sigma_u^-$ state should be related to direct creation of dications since, according to the calculations, the Auger processes lead to bound levels of this state. Structures 3 and 4 agree reasonably well with the 6.7 and 8.4 eV total kinetic energies released in unimolecular decomposition of O_2^{2+} in a fast

ion beam (Curtis and Boyd 1984). According to the calculations, the $v = 1$ levels of the $B'\,^3\Sigma_u^-$ and $B\,^3\Pi_g$ states have decay properties that make them suitable for detection by ion-kinetic-energy spectroscopy.

Structure 6 and the intensity extending to higher energies can be associated with dissociation from three electronic states as suggested in table 3. At 7 eV and above there are obviously additional transitions, which extend up to at least 10 eV and give rise to very broad bands in the ion spectrum. At 7 eV the $2^3\Pi_u \rightarrow O^+(^4S) + O^+(^2P)$ process may contribute to the spectrum. However, since the structure in the spectrum is very broad the dissociation process is probably primarily related to the direct double ionisation process.

Lines 1, 2 and 5 do not seem to correspond to dissociation from any of the doubly ionised states discussed in the present study. They could therefore be due to singly ionised molecules dissociating into an atom and an ion.

The photoionisation spectroscopy results of Eland *et al* (1988) are more difficult to understand. At a photon energy of 38 eV, they observed a total kinetic energy release of 4.5 eV, which, according to Eland *et al*, could only arise from ground state O_2^{2+} dissociating to ground state products. However, vibrational levels of the $X\,^1\Sigma_g^+$ state giving rise to only 4.5 eV kinetic energy are far from the top of the potential barrier and essentially stable. Furthermore, the 7.2 eV kinetic energy observed for a photon energy of 40.8 eV was ascribed to the $A\,^3\Sigma_u^+$ state. But, according to the calculations, excitation of the $A\,^3\Sigma_u^+$ state in the Franck–Condon zone would give rise to about 9.5 eV.

4. Conclusions

The core photoelectron, photon and electron beam excited Auger electron, autoionisation and ion fragment spectra of O_2 have been recorded with high resolution. The linewidths of the core O 1s $^4\Sigma^-$ and $^2\Sigma^-$ states are different indicating a larger equilibrium distance for the $^2\Sigma^-$ state. The Auger spectrum was assigned using CASSCF/MRCCI calculations of the potential curves for the doubly ionised states. The relationship between the Auger and the double charge transfer spectrum has been discussed. Two shake-up Auger satellites have been identified and a transition diagram has been established for the levels involved. The autoionisation lines in the Auger spectrum were identified by comparing the photon- and electron-beam-excited Auger electron spectra. The autoionisation spectrum was assigned using energies for singly ionised states in O_2^+. One of the autoionisation lines was, however, found to originate from a transition in a neutral core excited O atom. This neutral dissociation process has been discussed. The ion fragment spectrum has been discussed and a number of structures have been assigned with dissociation of the doubly ionised states via Coulomb explosion.

Acknowledgment

S Aksela, P J Fournier and D M Hanson are acknowledged for communicating unpublished results. This work was supported by the Swedish Natural Science Research Council.

Notes added in proof. Extended CI calculations by D M Hanson and co-workers (private communications) agree with our results suggesting that the $A\,^3\Sigma_u^+$ state is repulsive.

Additional experimental results on O_2^{2+} have been reported by Hamdan and Brenton (1989 *Chem. Phys. Lett.* **164** 413).

References

Ågren H, Selander L, Nordgren J, Nordling C, Siegbahn K and Müller J 1978 *Institute of Physics Report UUIP-982* Uppsala University

Ågren H, Selander L, Nordgren J, Nordling C, Siegbahn K and Müller J 1979 *Chem Phys.* **37** 161

Aksela H and Aksela S 1989 Private communication

Appell J, Durup J, Fehsenfeld F C and Fournier P 1973 *J. Phys. B: At. Mol. Phys.* **6** 197

Bagus P S, Schrenk M, Davis D W and Shirley D A 1974 *Phys. Rev.* A **9** 1090

Baltzer P, Karlsson L, Svensson S and Wannberg B 1989 *Institute of Physics Report UUIP-1209* Uppsala University

Baltzer P, Wannberg B, Svensson S and Karlsson L 1988 *Institute of Physics Report UUIP-1190* Uppsala University

Beebe N H F, Thulstrup E W and Andersen A 1976 *J. Chem. Phys.* **64** 2080

Besnard M J, Hellner L, Malinovich Y and Dujardin G 1986 *J. Chem. Phys.* **85** 1316

Beynon J H, Caprioli R M and Richardson J W 1971 *J. Am. Chem. Soc.* **93** 1852

Brehm B and de Frenes G 1978 *Int. J. Mass Spectrom. Ion Phys.* **26** 251

Cafolla A A, Reddish T and Comer J 1989 *J. Phys. B: At. Mol. Opt. Phys.* **22** L273

Carroll P K 1958 *Can. J. Phys.* **36** 1585

Carroll T X and Thomas T D 1989 *J. Chem. Phys.* **90** 3479

Chen M H, Crasemann B, Mårtensson N and Johansson B 1985 *Phys. Rev.* A **31** 556

Cosby P C, Möller R and Helm H 1983 *Phys. Rev.* A **28** 766

Cossart D, Bonneau B and Robbe J M 1987 *J. Mol. Spectrosc.* **125** 413

Cossart D and Launay F 1985 *J. Mol. Spectrosc.* **113** 159

Cossart D, Launay F, Robbe J M and Gandara G 1985 *J. Mol. Spectrosc.* **113** 142

Curtis D M and Eland J H D 1985 *Int. J. Mass Spectrom. Ion Phys.* **63** 241

Curtis J M and Boyd R K 1984 *J. Chem. Phys.* **81** 2991

Darko T, Hillier I H and Kendrick J 1977 *J. Chem. Phys.* **67** 1792

Dorman F H and Morrison J D 1963 *J. Chem. Phys.* **39** 1906

Dunlap B I, Mills P A and Ramaker D E 1981 *J. Chem. Phys.* **75** 300

Edqvist O, Lindholm E, Selin L E and Åsbrink L 1970 *Phys. Scr.* **1** 25

Eland J H D, Price S D, Cheney J C, Lablanquie P, Nenner I and Fournier P G 1988 *Phil. Trans. R. Soc.* A **324** 247

Fournier J, Fournier P G, Robbe J M, Gandara G and Langford M 1989 *J. Chem. Phys.* submitted and private communication

Gelius U 1973 *Institute of Physics Report UUIP-819* Uppsala University

Hitchcock A P and Brion C E 1980 *J. Electron Spectrosc* **18** 1

Huang K-N, Aoyagi M, Chen M H, Crasemann B and Mark H 1976 *At. Data Nucl. Data Tables* **18** 243

Hurley A C 1962 *J. Mol. Spectrosc.* **9** 18

Johansson B and Mårtensson N 1980 *Phys. Rev.* B **21** 4427

Johansson G, Hedman J, Berndtsson A, Klasson M and Nilsson R 1973 *J. Electron Spectrosc.* **2** 295

Jonathan N, Morris A, Okuda M, Ross K J and Smith D J 1974 *J. Chem. Soc. Faraday Trans. II* **70** 1810

Lie G C and Clementi E 1974 *J. Chem. Phys.* **60** 1275

Märk T O 1975 *J. Chem. Phys.* **63** 3731

Mathur M 1988 *Electronic and Atomic Collisions* ed H B Gilbody, W R Newell, F H Read and A C H Smith (Amsterdam: North-Holland) p 623

Moddeman W E, Carlson T A, Krause M O, Pullen B P, Bull W E and Schweitzer G K 1971 *J. Chem. Phys.* **55** 2317

Moore C 1949 *Atomic Energy Level* N B S Circular No 467 (Washington DC: US Govt Printing Office)

Morin P and Nenner I 1986 *Phys. Rev. Lett.* **56** 1913

Nordfors D, Nilsson A, Mårtensson N, Svensson S and Gelius U 1989 *Institute of Physics Report UUIP-1206* Uppsala University

Olsson B J, Kindvall G and Larsson M 1988 *J. Chem. Phys.* **88** 7501

Pedersen J O K 1986 *Electron Transfer to Multiply Charged Ions in Collisions between Atoms and Molecules* (Aarhus Institute of Physics, University of Aarhus)
Sambe H and Ramaker D E 1986 *Chem. Phys.* **104** 331
Sarre P 1989 Private communication
Siegbahn K, Nordling C, Johansson G, Hedman J, Heden P F, Hamrin K, Gelius U, Bergmark T, Werme L O, Manne R and Baer Y 1969 *ESCA applied to free molecules* (Amsterdam: North-Holland)
Siegbahn P E M 1983 *Int. J. Quantun. Chem.* **23** 1869
Siegbahn P E M, Almlöf J, Heiberg A and Roos B O 1981 *J. Chem. Phys.* **74** 2384
Svensson S, Eriksson B, Mårtensson N, Wendin G and Gelius U 1988 *Electron Spectrosc.* **47** 327
Svensson S, Karlsson L, Mårtensson N, Baltzer P and Wannberg B 1989 *J. Electron Spectrosc.* to be published
Tohji K, Hanson D M and Yang B X 1986 *J. Chem. Phys.* **85** 7492
van Duijneveldt F B 1971 *IBM Res. Repl RJ945*
Werme L O, Bergmark T and Siegbahn K 1973 *Phys. Scr.* **8** 149
Yang B X, Hanson D M and Tohji K 1988 *J. Chem. Phys.* **89** 1215
Yang H, Whitten J L and Hanson D M 1989 to be published